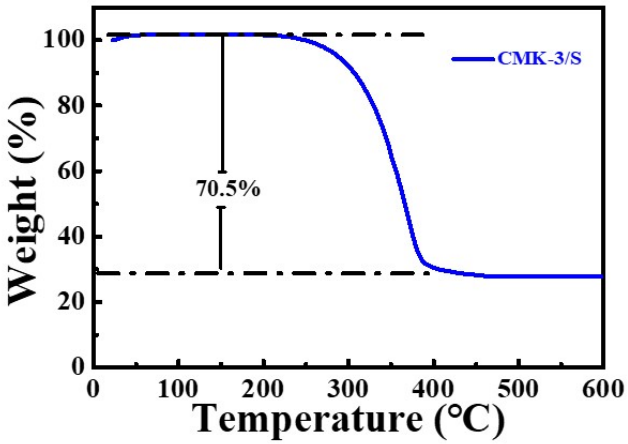

Fig. S1 TG curve of CMK-3/S composite material.

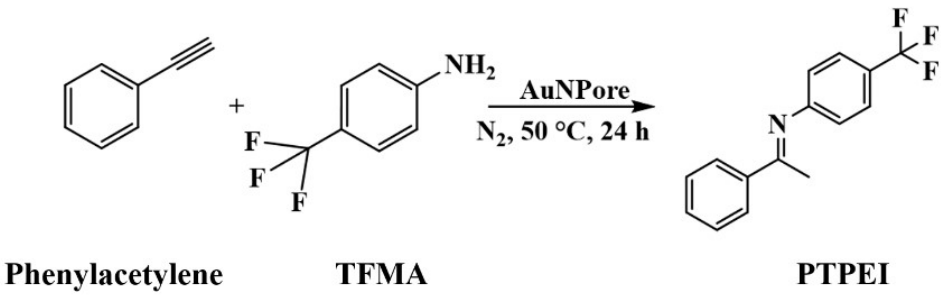

Fig. S2 Synthesis of PTPEI by hydroamination of TFMA.

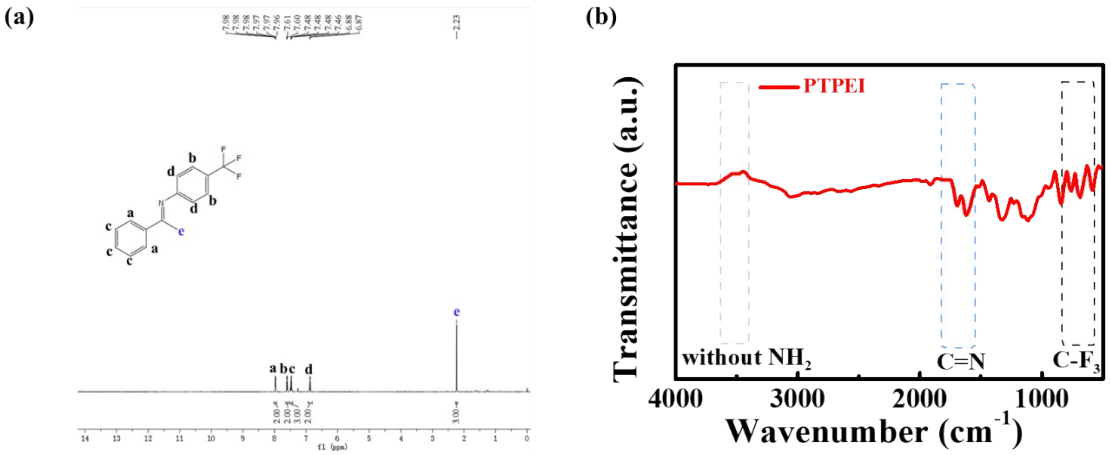

Fig. S3 (a) ^{1}H NMR spectra of the prepared PTPEI. (b) FTIR spectra of the prepared PTPEI.

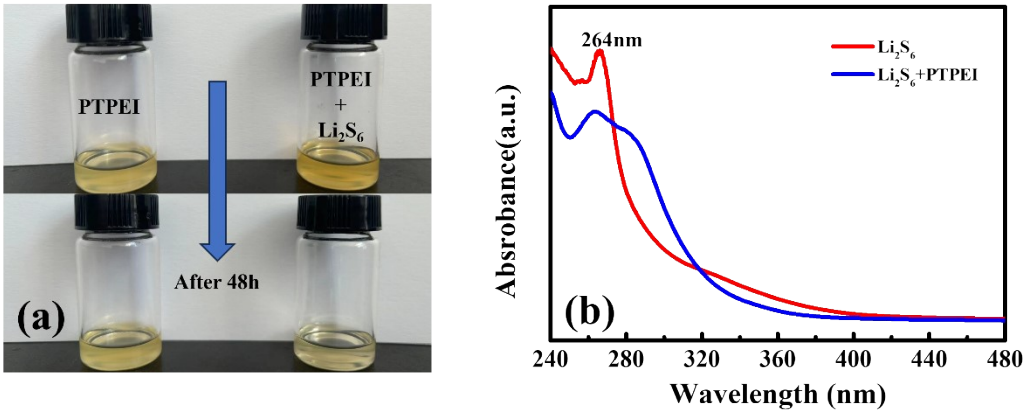

Fig. S4 (a) Visual reaction phenomenon between Li_2S_6 and PTPEI. (b) UV-visible spectra.

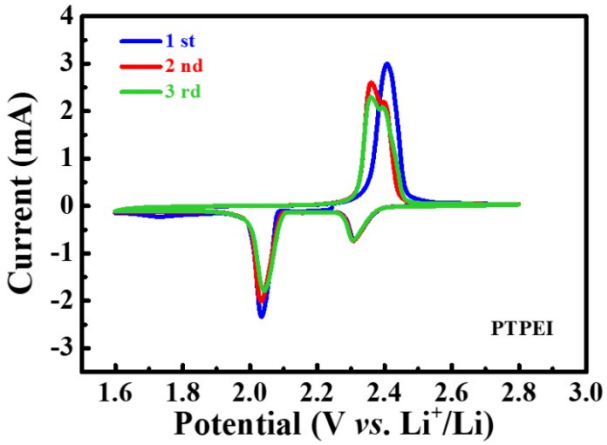

Fig. S5 First three cyclic voltammograms (CV) for the cell with PTPEI recorded at scan rate of 0.1 mV s^{-1} from 1.6 to 2.8 V.

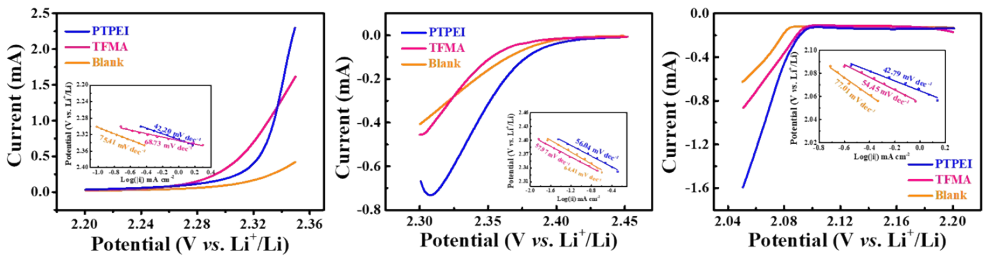

Fig. S6 CV profiles of various additives at a scan rate of 0.1 mV s^{-1} and Tafel plots.

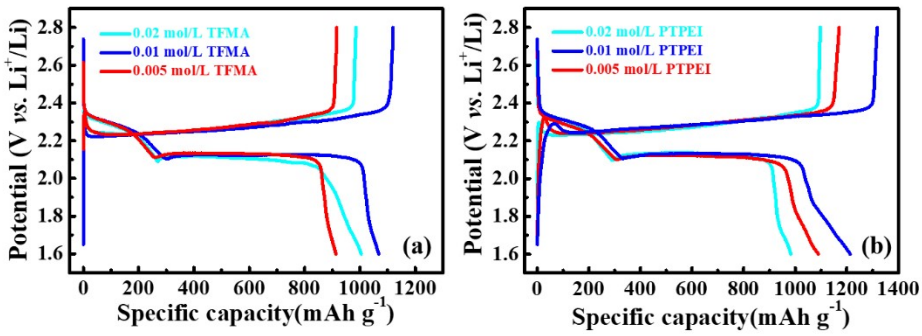

Fig. S7 Initial galvanostatic charge-discharge curves of the cells with different concentrations of (a) TFMA and (b)PTPEI at 0.1C.

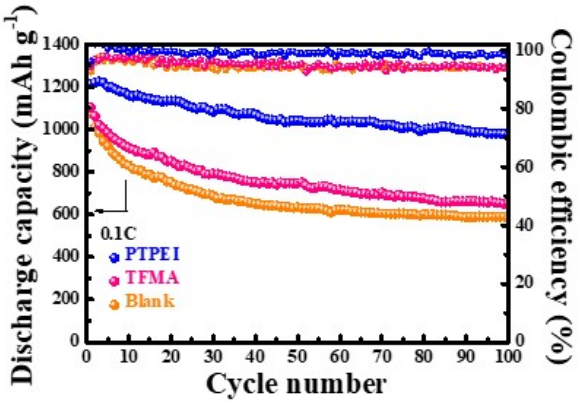

Fig. S8 Cycling of the cell with PTPEI, with TFMA, and with Blank at 0.1C for 100 cycles.

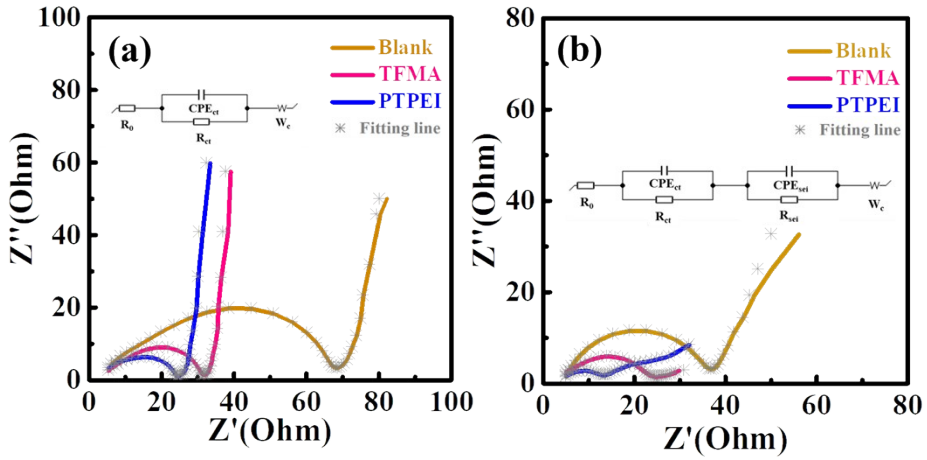

Fig. S9 Nyquist plots of the (a) pristine and (b) after 100 cycles cell with Blank, with TFMA, and with PTPEI at 0.1C.

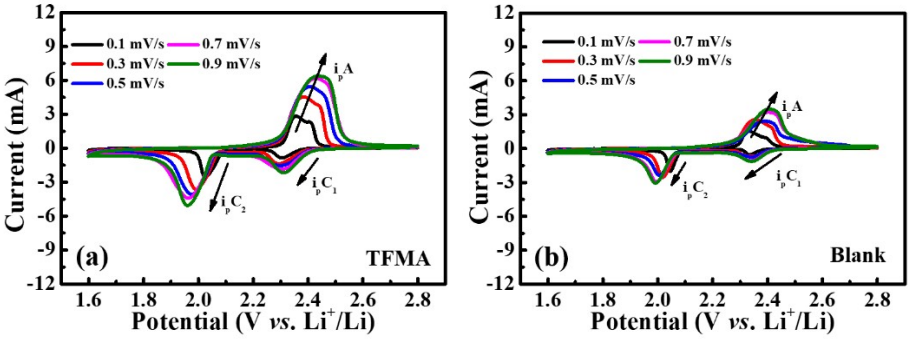

Fig. S10 CV curves of the cell (a) with TFMA and (b) with Blank at different scanning rate from 0.1 to 0.9 mV s^{-1}.

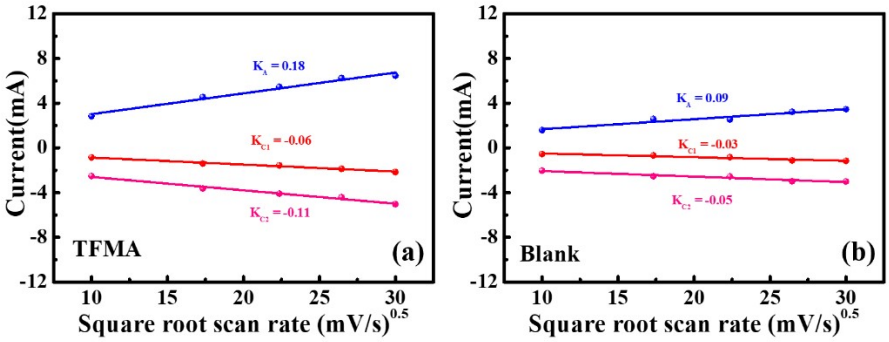

Fig. S11 Plot of Li^+ ion diffusion kinetics for cell (a) with TFMA and (b) with Blank.

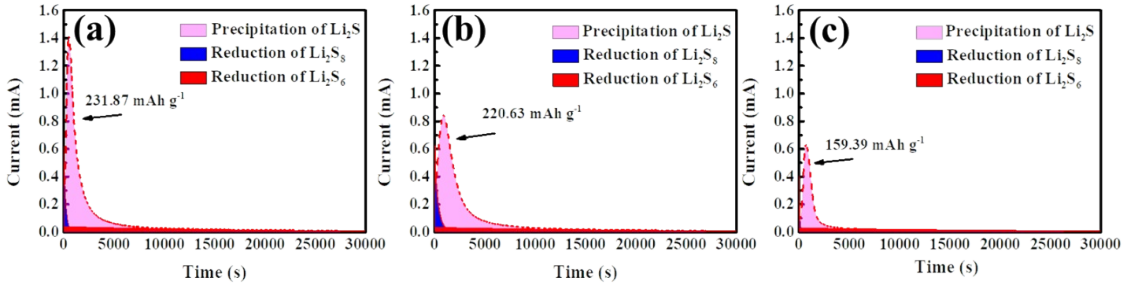

Fig. S12 Potentiostatic discharge profiles of Li_2S deposition (a) with PTPEI (b) with TFMA and (c) with Blank.

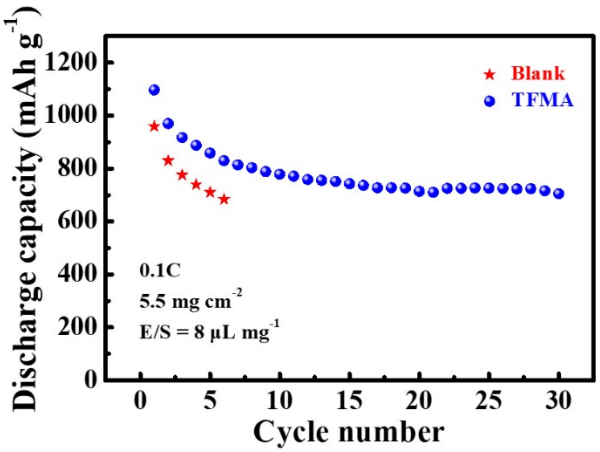

Fig. S13 Cycling of the cell with Blank and with TFMA at a high sulfur loading (5.5 mg cm^{-2}) and a low E/S ratio (8 µL mg^{-1}) at 0.1C.

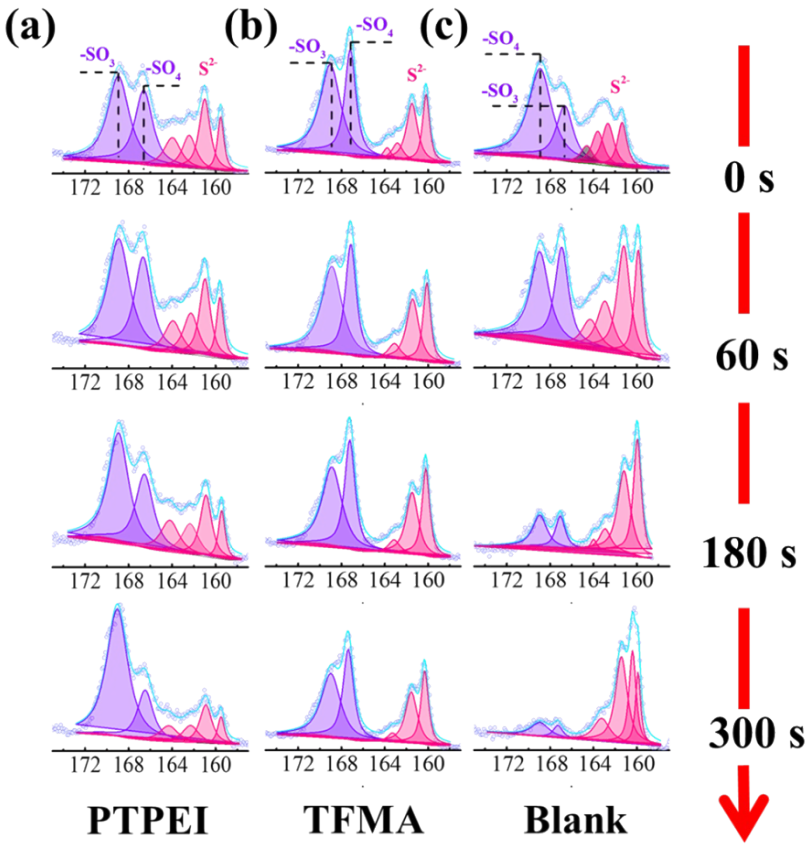

Fig. S14 XPS spectra with different depth etch on the surface of Li-anode for Li-S cells after 100 cycles at 0.1C. S 2p spectra corresponding to the cell (a) with PTPEI, (b) with TFMA, and (c) with Blank.

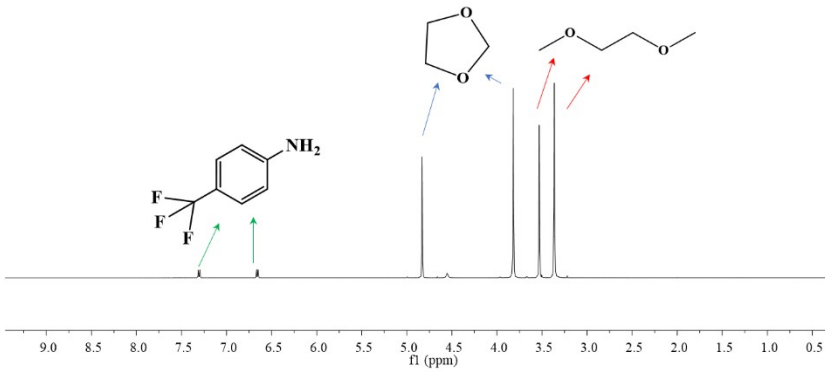

Fig. S15 ^{1}H NMR spectra of the SEI from the cell with TFMA after 100 cycles.

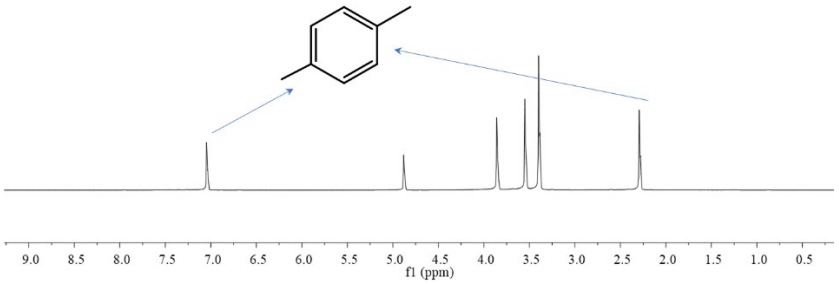

Fig. S16 ^{1}H NMR spectra of the SEI from the cell with PTPEI after 100 cycles.

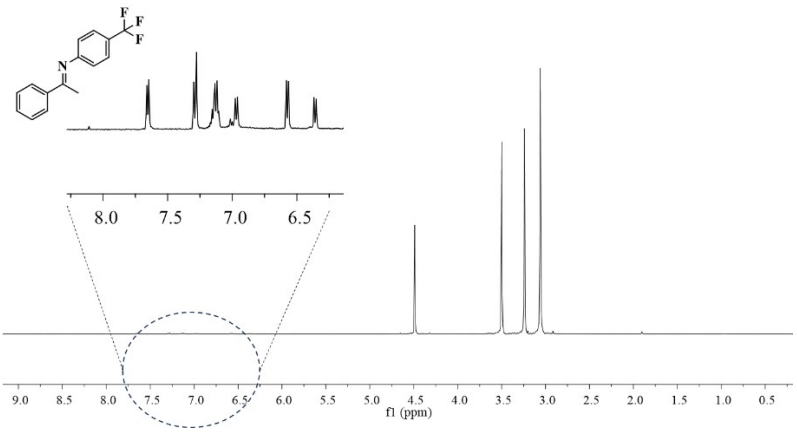

Fig. S17 ^{1}H NMR spectra of the electrolyte from the cell with PTPEI after 100 cycles.

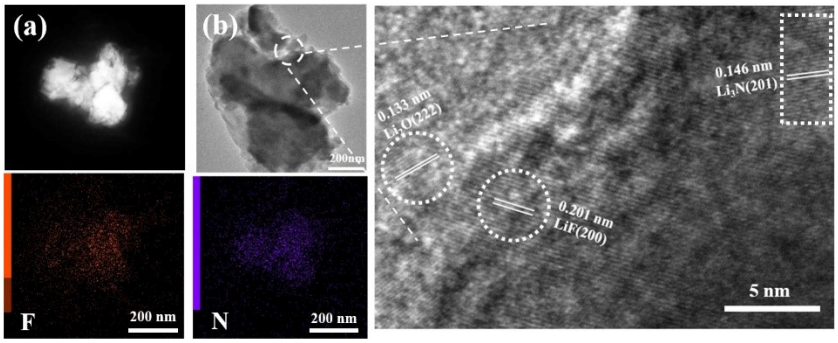

Fig. S18 TEM, HRTEM, and elemental mapping images of the SEI from the cell with PTPEI.

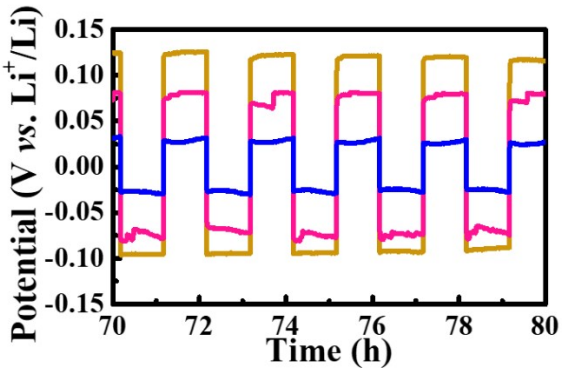

Fig. S19 The voltage profiles of Li || Li symmetric cells with PTPEI, with TFMA, and with Blank at a current density of 1 mA cm^{-2} from 70 to 80 h.

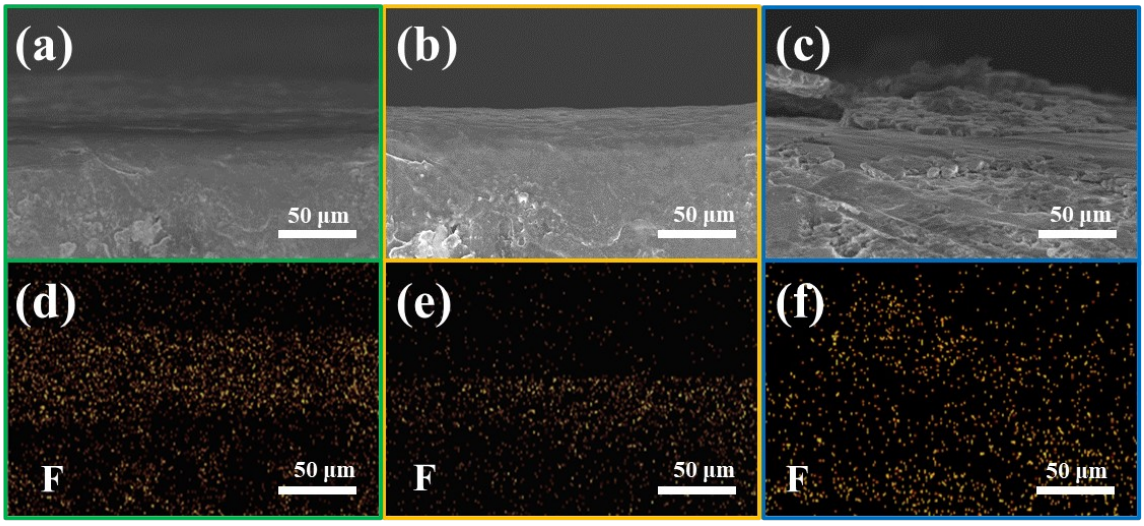

Fig. S20 SEM images of (a-c) cross-section, and (d-f) EDS elemental mapping profiles for the Li-metals from Li || Li symmetric cells with PTPEI, cell with TFMA, and cell with Blank after 20 h, respectively.

Table. S1 The data of the equivalent circuit fitting analysis.

	Pristine			After 100 cycles		
Additives	PTPEI	TFMA	Blank	PTPEI	TFMA	Blank
$R_0(\Omega)$	5.35	5.40	6.13	5.03	5.06	5.08
R_{ct} (Ω)	18.63	26.69	62.14	11.18	18.85	30.82
CPE_{ct}	2.02×10^{-6}	1.74×10^{-6}	1.53×10^{-6}	7.12×10^{-6}	6.53×10^{-6}	5.27×10^{-6}
R_{sei} (Ω)	-	-	-	3.03	5.07	9.23
CPE_{sei}	-	-	-	5.34×10^{-5}	4.11×10^{-5}	3.31×10^{-5}
σ_w (Ω $s^{-1/2}$)	19.94	24.03	31.17	12.76	19.11	25.23

R_0 represents the ohmic resistance of the battery, including the electrolyte and electrodes. R_{sei} and CPE_{sei} are the resistance and constant phase element (CPE) associated with the passive layer, respectively. R_{ct} and CPE_{ct} are related to charge transfer. σ_w is the Warburg contribution taken at the infinite limit.

Table. S2 The specific data related to the calculation of $D_{(Li^+)}$ for the studied systems.

Element	A		C_1		C_2	
	Slope	$D_{(Li^+)}$	Slope	$D_{(Li^+)}$	Slope	$D_{(Li^+)}$
PTPEI	0.24	3.01×10^{-7}	-0.16	2.45×10^{-7}	-0.20	2.75×10^{-7}
TFMA	0.18	2.60×10^{-7}	-0.06	1.50×10^{-7}	-0.11	2.03×10^{-7}
Blank	0.09	1.84×10^{-7}	-0.03	1.06×10^{-7}	-0.05	1.37×10^{-7}

Table. S3 Comparison of the performances of Li-S batteries with different electrolyte additive.

Additive and Dosages	Electrolyte	Capacity ($mAh\ g^{-1}$)	Capacity retention	Journal	Reference
1% phenyl-1-(4-trifluoromethyl)phenyl)ethan-1-imine （PTPEI）	1 M LiTFSI DME/DOL(1:1 vol%) +1 wt% $LiNO_3$	1190.9-645.9 (5.5 mg cm^{-2} 0.1C 1^{st}-50^{th}) 1214-981.2 (1.4 mg cm^{-2} 0.1C 1^{st}-100^{th}) 1178.8-580 (1.4 mg cm^{-2} 1C 1^{st}-200^{th})	**54.2%** **80.8%** **49.2%**	This work	
lanthanum nitrate ($La(NO_3)_3$)	1 M LiTFSI DME/DOL(1:1 vol%) +2 wt% $LiNO_3$	912-553 (0.9 mg cm^{-2} 0.2 C 10^{th}-100^{th})	**64.2%**	ACS Appl. Mater. Interfaces	[1]
2% Thioacetamide (TAA)	1 M LiTFSI DME/DOL(1:1 vol%) +2 wt% $LiNO_3$	1148.6-738.9 (1.2 mg cm^{-2} 0.5 C 1^{st}-200^{th})	**64.3%**	Electrochim. Acta	[2]
2% Yttrium nitrate ($Y(NO_3)_3$)	1 M LiTFSI DME/DOL(1:1 vol%) +1 wt% $LiNO_3$	911.7-711.9 (1.2 mg cm^{-2} - 1.5 mg cm^{-2} 0.5 C 1^{st}-250^{th})	**78.1%**	ACS. Sustain. Chem. Eng	[3]
0.1M Thiophene	1 M LiTFSI DME/DOL(1:1	1016-751.8 (3.6 mg cm^{-2} 0.025 C 1^{st}-100^{th})	**74%**	J. Power Sources	[4]

	vol%) +2 wt% $LiNO_3$				
2% 4,4-thiodibenzenethiol (TBBT)	1 M LiTFSI DME/DOL(1:1 vol%) +2 wt% $LiNO_3$	994.4-752.7 (1-1.5 mg cm^{-2} 0.5 C 1^{st}-300^{th})	**75.6%**	Mater. Chem. Front	[5]
0.05 M Diphenyl Ditelluride (DPDTe)	1 M LiTFSI DME/DOL(1:1 vol%) +2 wt% $LiNO_3$	1142.2-640.4 (5 mg cm^{-2} 0.1 C 1^{st}-100^{th})	**56%**	Energy Environ. Mater.	[6]
0.1M Diphenyl Diselenide (DPDSe)	1 M LiTFSI DME/DOL(1:1 vol%) +2 wt% $LiNO_3$	924-765 (5 mg cm^{-2} 0.1 C 1^{st}-55^{th})	**82%**	Adv. Mater.	[7]

Table. S4 The value of energy levels of FMOs for Li_2S_x - PTPEI, Li_2S_x - TFMA and Li_2S_x (x = 1, 2, 4, 6, and 8).

	Li_2S_x - PTPEI			Li_2S_x - TFMA			Li_2S_x		
	LUMO	HOMO	Δ*E*	LUMO	HOMO	Δ*E*	LUMO	HOMO	Δ*E*
Li_2S	-0.08	-5.72	5.64	0	-5.65	5.65	-0.08	-6.29	6.21
Li_2S_2	0.04	-6.20	6.24	0.09	-6.72	6.81	0.02	-6.68	6.70
Li_2S_4	-0.04	-7.29	7.25	0.12	-7.51	7.63	0.01	-8.04	8.05
Li_2S_6	-0.34	-7.88	7.54	-0.21	-7.80	7.69	-0.56	-8.12	7.56
Li_2S_8	-0.42	-7.62	7.20	-0.66	-7.87	7.21	-0.89	-8.21	7.32

References:

[1] S. Liu, G. R. Li, X. P. Gao, ACS Appl. Mater. Interfaces 2016, 8, 7783-7789.

[2] J. Li, L. He, F. Qin, J Fang, B. Hong, Y. Lai, Electrochimica Acta, 2021, 376: 138041.

[3] X. Hao, Y. Mao, T. Zhu, Y. Liu, T. Li, Y. Xiao, J. Zang, W. Wang, Y. Li, J. Ding, ACS Sustainable Chemistry & Engineering, 2024, 12(9): 3691-3701.

[4] S. Lee, K. Sim, K. Y. Cho, S Kim, K. S. Eom, Journal of Power Sources, 2023, 582: 233517.

[5] C. Y. Shi, S. Y. Shao, C. X. Zong, J. H. Gu, Z. Y. Huang, Q. Y. Wang, B. Hong, M. R. Wang, Z. A. Zhang, J. Li, Y. Q. Lai, Materials Chemistry Frontiers, 2023, 7(1): 145-152.

[6] W. Zhang, F. F. Ma, Q. Wu, Z. Q. Zeng, W. Zhong, S. J. Cheng, X. Chen, X. Jia, Energy & Environmental Materials, 2023, 6(3): e12369.

[7] M. Zhao, X. Chen, X. Y. Li, B. Q. Li, J. Q. Huang, Advanced Materials, 2021, 33(13): 2007298.